Developing a Flapping Gear System for Butterfly-Inspired Motion

Frederick Schulze[1] and Chang-kwon Kang[2]
University of Alabama in Huntsville, Huntsville, Alabama, 35899

Bioinspired flapping-wing drones have the potential to revolutionize data collection techniques with increased versatility and performance over existing rotary and fixed-wing drone types. Their capability for increased power efficiency is demonstrated in the long-range migration of Monarch butterflies. However, the wing motion is more complicated, resulting in three-dimensional wing kinematics. To better understand the performance of these wings, a flapping wing gear system is developed to reproduce the flapping motion of a monarch butterfly. The mechanism consists of a two-stage gear reduction and a 4-bar linkage to convert rotary motion to flapping motion. A dynamic analysis performed on the proposed gear system shows that the flapping wing amplitude and frequency depend on the rpm of the motor, gear ratios used, and the lengths of the linkages making up the system. Simulations with variations of these characteristics were performed to create a flapping mechanism that mimicked butterfly flapping as closely as possible. The resulting flapper design achieved a range of motion comparable to a monarch butterfly with smooth sinusoidal motion.

I. Nomenclature

R_1	=	main axis arm	[mm]
R_2	=	driving arm	[mm]
R_3	=	arm connecting drive gear to wing arm	[mm]
R_4	=	wing arm	[mm]
S	=	imaginary line from R_4/R_1 joint to R_2/R_3 joint	[mm]
S_1	=	imaginary line from R_4/R_1 joint to R_2 joint at center of gear	[mm]
$R\phi$	=	imaginary line from tip of R_1 to center of gear	[mm]
θ_2	=	angle of R_2 with respect to S_1	[deg]
θ_3	=	angle of R_3 with respect to S_1	[deg]
θ_4	=	angle of R_4 with respect to S_1	[deg]
ω_2	=	angular velocity of R_2	[deg/s]
ω_3	=	angular velocity of R_3	[deg/s]
ω_4	=	angular velocity of R_4	[deg/s]
α_2	=	angular acceleration of R_2	[deg/s^2]
α_3	=	angular acceleration of R_3	[deg/s^2]
α_4	=	angular acceleration of R_4	[deg/s^2]
α	=	angle between S_1 and R_1	[deg]
β	=	angle between S and S_1	[deg]
λ	=	angle between R_4 and S	[deg]
ψ	=	angle between R_3 and S	[deg]
ϕ	=	angle between R_1 and rϕ	[deg]
R	=	wing length from axis of rotation to wing tip	[mm]

[1] Undergraduate Student Researcher, Department of Mechanical and Aerospace Engineering, 301 Sparkman Drive, Huntsville, Alabama 35899, AIAA Student Member
[2] Associate Professor, Department of Mechanical and Aerospace Engineering, 301 Sparkman Drive, Huntsville, Alabama 35899, AIAA Associate Fellow

II. Introduction

Drone usage has increased dramatically in the past decade alongside the development of cheaper and more advanced drones. Rotary-wing and fixed-wing drones have become developed to such an extent that their room for improvement has diminished. However, flapping wing drones are still not well understood, and have an unrealized potential. Rotary wing drones can hover well but struggle with traveling at high speeds with efficiency. Fixed wing drones can travel efficiently at high speed but lack the ability to hover. Flapping wing drones may offer the increased versatility of being able to accomplish both high-speed travel and hovering efficiently.

In nature, flapping wings are the solution to being able to do all these things effectively – flying at low and high speeds while being able to take off and land in small spaces. The monarch butterfly is a prime example of an insect that uses flapping wings for efficient travel. Monarchs migrate up to 3,000 km [1] every year and have evolved to do so with exceptional efficiency. If these principles can be applied to flapping drone development, high efficiencies may be able to be achieved. However, at this time, the unsteady aerodynamics of flapping wings is still not adequately understood.

To better understand the performance of these wing motions, monarch butterfly wings were tested. The goal was primarily to analyze deformation of the wing, forces produced by flapping, the effects of flapping frequency. To accomplish this, a monarch forewing was attached to a flapping mechanism emulating a butterfly's flapping motion. A Vicon 3D motion capture system was used to track markers placed on the monarch wing (Figure 1). A force balance was also used to record the forces produced by the butterfly during flapping. When the data from these two instruments was pieced together, it was found that the maximum lift occurred at close to 10 Hz, which is close to the frequency that monarch butterflies flap at to produce maximum lift. The deformation also increased as flapping frequency increased.

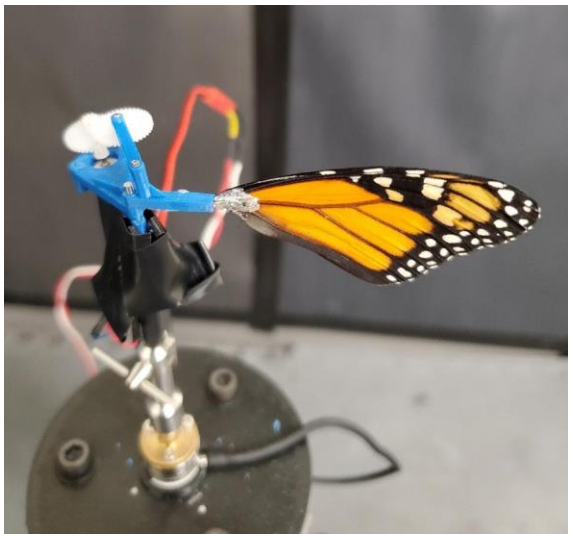

Figure 1. Monarch Butterfly Wing set up for Testing on Force Balance

However, the objective of this paper is to report on the development of a butterfly-inspired flapping mechanism. This flapper was designed to produce similar flapping motion to a monarch butterfly and allow monarch wings or artificial wings to be attached to the end of it. An experimental observation [**Insert a Ref here]** showed that butterfly wings undergo a sinusoidal flapping motion with an amplitude of 75 degrees where 15 degrees of this range is due to the wing deformation at a frequency of 10 Hz. The developed gear system was able to flap with a similar frequency and range of motion to a monarch butterfly. An analysis of the dynamics of this system is performed with analytical and numerical techniques to determine motion of every moving part, and ultimately the motion of the flapping wing.

This report includes a breakdown of the design of the gear system, methods and used for the dynamic analysis, and resulting motion of the mechanism, determined both analytically and experimentally.

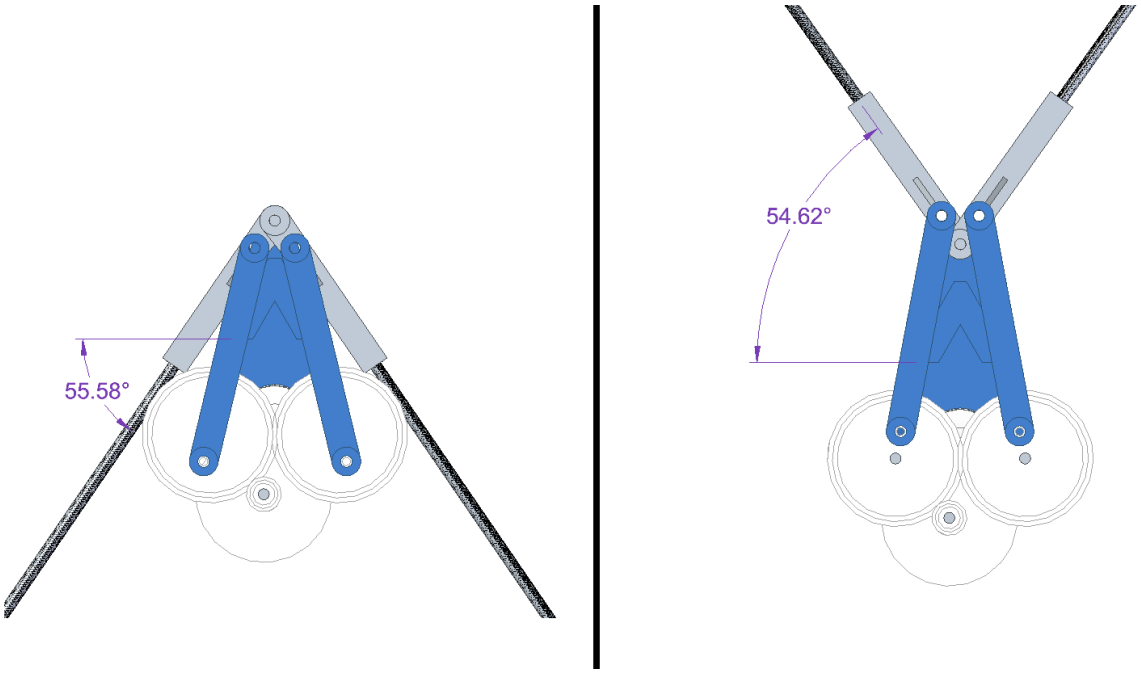

Figure 2. Range of motion of developed mechanism

III. Methodology

A. Design of the Gear System

The goal of the gear system is to convert the rotary motion of the motor into flapping motion. This is accomplished by using a four-bar linkage along with a gear reduction. The core of the flapping mechanism is single main frame piece to which all parts are attached. There is small pinion gear for the motor, an intermediate gear that increases the gear ratio, and a large output gear that further increases the total gear ratio of the mechanism. The result is that two 5:1 gear ratios produce a total 25:1 gear reduction between the driving motor and flapping mechanism. This is necessary because the electric motor best operating revolutions per minute (RPMs) are much higher than the desired flapping frequency of the flapper. To achieve the butterfly's flapping frequency of 10Hz, the motor operates at 3000 RPM, which is comfortably within the ideal operating range of the motor. Figure 1 shows the completed flapper assembly without an attached wing. The individual parts can be seen in more detail below in Table 2:

Table 1. Parts of four-bar linkage mechanism

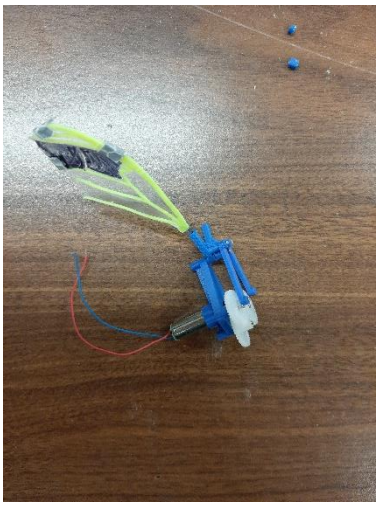

Figure 3. Manufactured gear system

			
Frame	Driving Gear	Gear Linkage	Flapping Arm

The importance of the frame is to position all the parts in their correct places. For the gears and motor, this is simply based on the gear size to achieve good meshing between the gears. However, for the flapping arm, the placement of its axis of rotation is crucial for achieving a certain range of flapping motion. Placing it lower makes for better flapping because linkages can push at angles normal to each other rather than opposing each other. However, to even be able to achieve a high range of motion, the arm had to be placed far away from the gears to give the wing room to flap. Otherwise, the wing would hit the main frame on the downstroke.

One additional feature of the frame is the upside-down V-shaped protrusion in the middle. This is a bump stop, added to prevent overextension of certain linkages. Due to the high range of motion and inertia of the wing, there is a risk of overextension, especially on the downstroke, which results in the mechanism locking up. With this piece added, if the wing starts to overextend, it hits the limiter preventing it from going too far.

The length of the gear linkage needs to be tuned to get a symmetrical range of motion with respect to horizontal (for example, +60/-60 . The length has a very minor effect on the total range of motion but shifts the limits up or down depending on the length of the linkage. A longer length will shift both the upper and lower flapping limits upwards, while a shorter length shifts both the upper and lower flapping limits downwards.

Flapping amplitude, or total range of motion, is largely determined by where the gear linkage connects to both the flapping arm and driving gear. On the gear, the radial distance of the joint determines how much the rest of the mechanism is going to move. The larger the radial distance, the larger the flapping amplitude. However, on the flapping arm, moving the connection point farther away from the axis of rotation decreases the flapping amplitude. This is because the gear linkage is going to move up a set amount with each gear rotation, meaning that there is an inverse relationship between arm length and angular displacement. The gears were prefabricated, so this piece was tuned to achieve the desired 120-degree range of motion.

B. Dynamic Analysis

The decomposition of the gear system as a four-bar linkage allows for detailed dynamic analysis of its mechanics. Linkages S_1, R_1, and R_Φ are all considered to be fixed, as these are imaginary lines connecting the axes of rotation of different parts on the main frame. Thus, only linkages R_2, R_3, and R_4 are moving. Linkage R_2 is the linkage that is drawn from the center of the gear to a point on the gear where R_3 attaches. The R_3 linkage connects the gear to the flapping arm and serves to convert the rotational motion of the R_2 gear linkage to oscillating motion of the R_4 linkage. The R_4 linkage is what the wing attaches to, so the results will be focused on the motion of this linkage to determine wing motion.

The variable resistance created by flapping has a negligible effect on motor speed, so it is reasonable to assume that R_2 rotates at a constant angular velocity. This linkage acts as a driving linkage for the rest of the four-bar linkage, with the movement of R_3 and R_4 being dependent on R_2. Therefore, all analysis will be focused on comparing outputs to the independent variable θ_2, which is the angle of R_2 with respect to S_1.

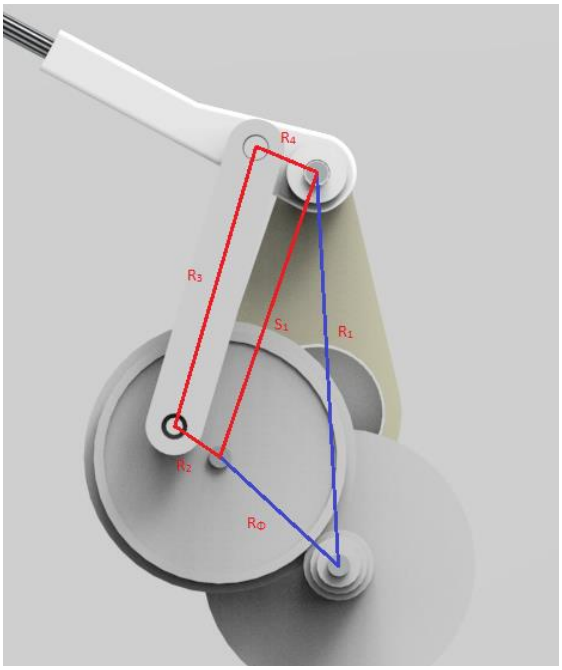

Figure 4. CAD rendering of four-bar linkage flapping mechanism

The method used to calculate dynamic parameters of the flapper involves using known lengths of linkages and the known constant angular velocity of R_2. Law of sines must be used to calculate S, an imaginary line drawn across the four-bar linkage that simplifies the quadrilateral into 2 triangles. Law of cosines is used to calculate the angles within these triangles. These can then be used to calculate the angles of all the different linkages. The relationship between linkage R_4 and R_2 is the most important to understand because it relates the driving gear to the flapping wing.

The process for calculating the position and angle of the linkages at any point during the flapping cycle will now be detailed. First, the four-bar linkage can be simplified into just two triangles which will make the rest of the geometry solvable with just trigonometry. Law of Cosines is used to solve for the length S as shown in equation 1, where S_1 is length of the stationary body linkage, R_2 is length of the gear linkage, θ_2 is angle of R_2 with respect to S_1, and S is length of the resulting linkage.

$$S = \sqrt{S_1^2 + R_2^2 - 2S_1 r_2 cos\theta_2} \tag{1}$$

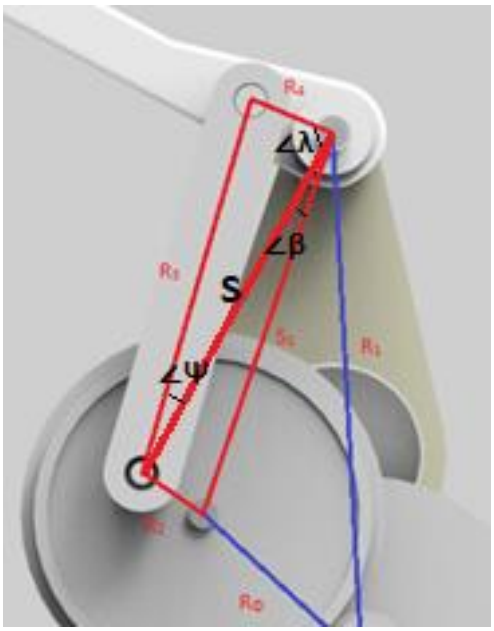

Figure 5. Four-bar linkage simplified to two triangles

This simplifies the rest of the system to a triangle, which can be solved for relatively easily. Linkage lengths are all known this time, so Law of Cosines is applied again, except this time to solve for the angles of the triangle. This calculation is shown in equation 2 where ψ is the angle of R_3 with respect to S, and R_3, S, and R_4 are lengths of linkages shown above in Figure 5.

$$\psi = \cos^{-1}\left(\frac{R_3^2 + S^2 - R_4^2}{2 \cdot R_3 \cdot S}\right) \tag{2}$$

However, this triangle's orientation with respect to the original 4-bar-linkage needs to be known. This is found in a similar fashion using equation 3, where R_1, S, and R_2 are linkage lengths, and β is the angle of S with respect to S_1:

$$\beta = \cos^{-1}\left(\frac{R_1^2 + S^2 - R_2^2}{2 \cdot S \cdot R_1}\right) \tag{3}$$

A similar process can be used to find all angles within these two triangles, but due to the nature of crossing linkages, two solutions are always yielded. In order to determine the correct solution, the conditional statement in equation 4 is used, where θ_i is the angle of R_i with respect to S_1, and other variables are angles illustrated above in Figure 5.

$$\begin{gathered} if\ \theta_2 \leq 180, \theta_3 = -\beta + \psi, \theta_4 = 180 - \beta - \lambda \\ if\ \theta_2 \geq 180, \theta_3 = \beta + \psi, \theta_4 = 180 + \beta - \lambda \end{gathered} \tag{4}$$

These angles of all linkages are calculated for all values of the independent variable θ_2 within the range $0 \leq \theta_2 \leq 360$ with a step size of 0.1 to determine the state of the system at any point during a flapping cycle. The angular velocities can be found numerically using the method demonstrated in equation 5 where ω_i is the angular velocity of linkage i, and θ_i is the angle of linkage i with respect to linkage S_1:

$$\omega_i = \frac{d\theta}{dt} = \frac{\theta_{i+1} - \theta_i}{t_{i+1} - t_i} \tag{5}$$

Angular acceleration can be found in the same exact fashion as equation 5, as demonstrated in equation 6 below, where α_i is angular acceleration of linkage i, and ω_i is the angular velocity of linkage i.

$$\alpha_i = \frac{d\omega}{dt} = \frac{\omega_{i+1} - \omega_i}{t_{i+1} - t_i} \tag{6}$$

At this point, all angles, angular velocities, and angular accelerations are found as a function of time through a hybrid analytical and numerical process. Finding the locations of specific points such as connections of linkages, or the tip of the wing is a matter of simple vector addition which does not need its own detailed discussion.

C. Testing with Vicon Motion Capture System

The goal of creating this flapping gear system was to use it to analyze the performance of wings and gain a better understanding of biological flapping wing dynamics. To do this, both artificial and real monarch wings were attached to the flapper in the experimental setup pictured below in Figure 6. The flapper was placed on a force balance which recorded forces and moments in all 3 axes during flapping. A Vicon 3D Motion Capture system was used to track the position of the wing as it flapped at various frequencies including the monarch butterfly's flapping frequency of 10Hz. The cameras work by using infrared signals to detect the distance of a reflective marker (about 1mm in diameter). A single camera sees a 2D image, but multiple cameras used together can determine the position of these markers in 3D space.

Figure 6: Vicon 3D motion tracking setup

The setup can simultaneously track position of the wing and forces generated, but analysis of wing performance is not in the scope of this paper. To determine the flapper's success in imitating butterfly motion, only angle of the wing over time is needed. To track the motion of the flapper, three markers were placed on the monarch wing and two on the test stand for the flapper. The two markers on the body are stationary and in a vertical line so that the wing markers' position relative to a vertical axis can be obtained [2]. The three markers on the wing can be used to define a plane, and this plane's angle over time relative to a stationary plane can be determined. Once processed, this angle over time of the wing can be compared to the angle over time predicted by the dynamic analysis.

IV. Results and Discussion

The resulting angle over time from the dynamic analysis of the flapper is shown below in Figure 7. By adding the total angular displacement on both the upper and lower ends, a total range of motion of 118.15° is obtained, which is very close to the goal of 120° and within the acceptable bounds of error, considering a manufactured design would likely have imperfections. The flapping angle time history also appears to be mostly sinusoidal in nature when observing the position and angle plots. However, it can be seen in the first plot of angle over time that there is a somewhat sharp turn at the upper and lower limits. Any deviation from smooth sinusoidal motion is further revealed in the velocity and acceleration plots of both angle and position, as these differences are amplified once the derivative is taken.

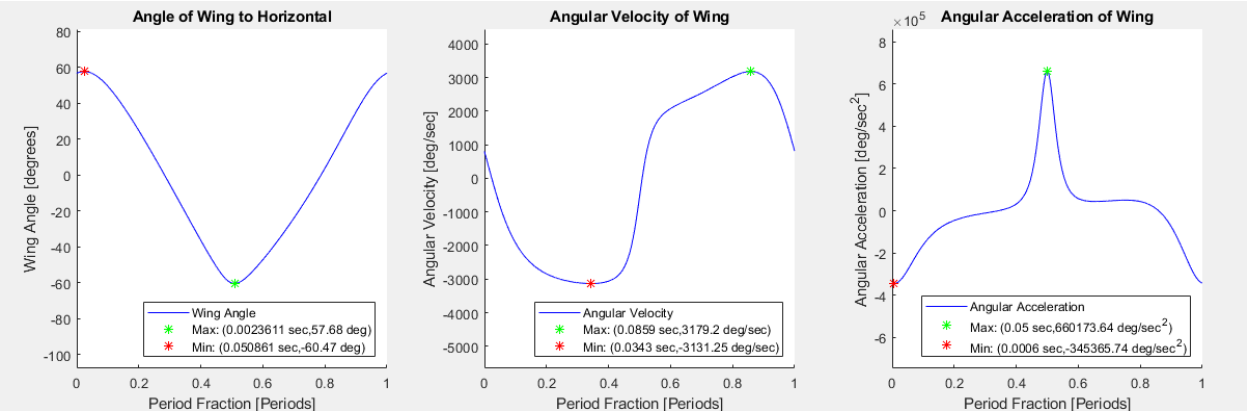

Figure 7: Wing angle, angular velocity, and angular acceleration over time

The manufactured flapper was able to flap fluidly through a large range of motion. The following frames shown in Figure 8 were from a video taken of the flapper. These demonstrate the ability of the flapper to flap through its whole range of motion at a very high frequency (up to 20 Hz tested).

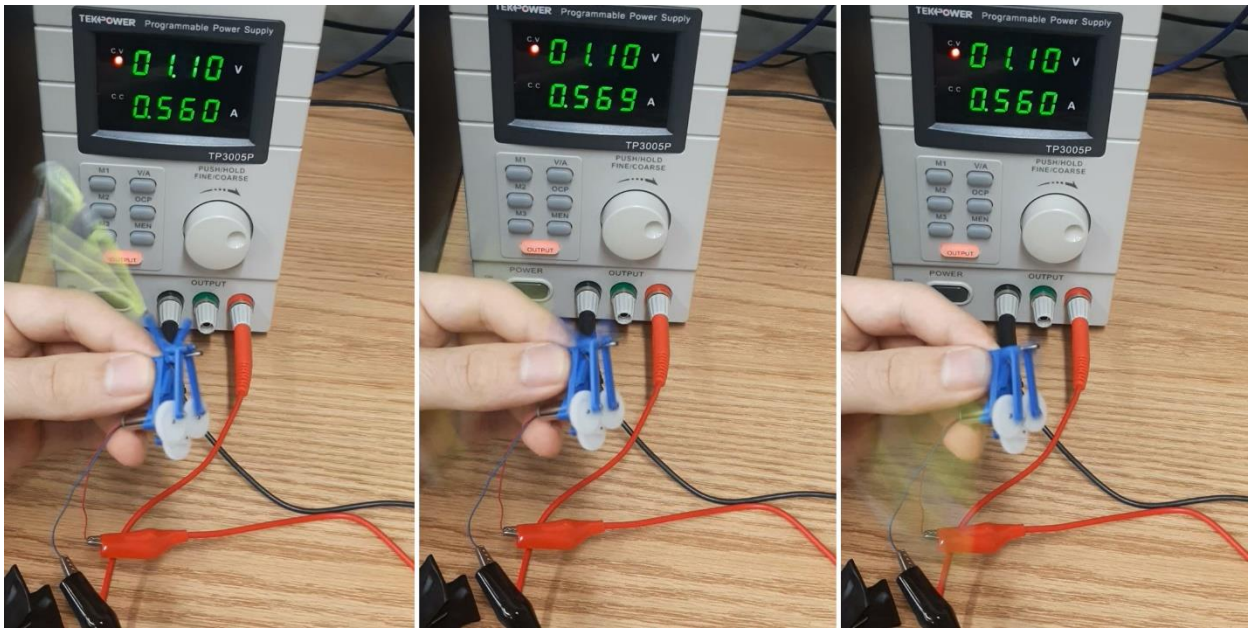

Figure 8. Snapshots showing high range of motion flapping

The motion recorded by the Vicon camera system revealed a total flapping amplitude of 91.41° (Figure 8). This was measured at a voltage of 0.7V to the motor, as this was the test that most closely matched the flapping frequency of a butterfly (9.45 Hz in the test vs 10Hz of a monarch butterfly). The flapping frequency of the motor increases almost proportionately with input voltage. This number contradicts the flapping amplitude prediction of 118.15°. This can be largely attributed to deformation of the wing under its own inertia and aerodynamic forces. Since the markers on the wing were used to record this flapping angle, deformation of the wing will certainly affect the result. Additionally, this is likely partially due to inertia of the wing causing flex in the mechanism due to imperfections with FDM-type 3D printing. The asymmetry about the horizontal line in the figure should not be a cause for concern, because with the way the angle is calculated, the plane of reference is arbitrary, and total motion is more important. While is appears that the flapping angle ranges from -70 to +20, further analysis would have to be performed to test if the motion is symmetrical.

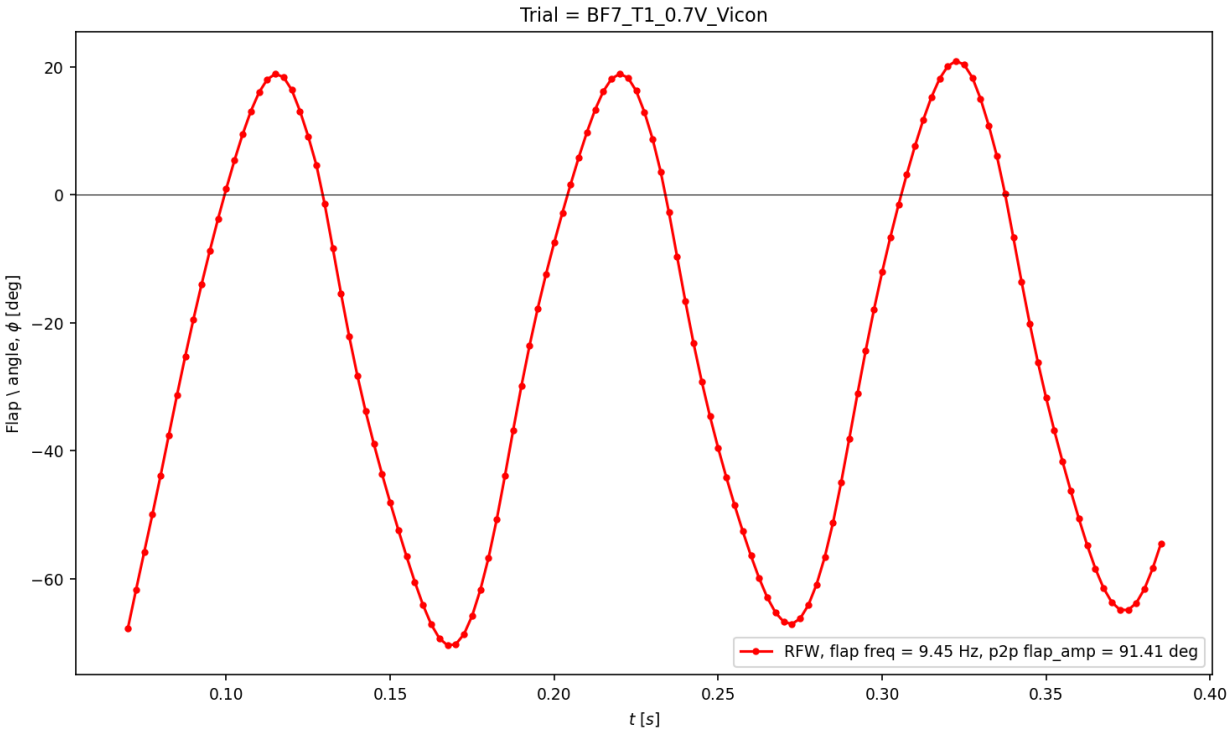

Figure 9. Wing over time measured by Vicon cameras

V. Concluding Remarks

The objective of this study was to develop a better understanding of the four-bar linkage based flapping mechanism used in this design and create motion as close as possible to a butterfly. In the analysis of the flapping mechanism, we gained a better understanding of how each component of the four-bar linkage can affect the resulting motion. This will allow for faster development of similar mechanisms with different desired flapping characteristics. The current prototype provides the ability to test different the performance of different bioinspired wings with dynamics similar to a butterfly. Consequently, this experiment can be considered a success. We will want to continue to refine this mechanism to see if its motion can be tuned to match a butterfly even more closely. The next steps are to test artificial wings based on bioinspired wings and compare their performance to real monarch wings.

Acknowledgements

I would like to thank Dr. Chang-Kwon Kang and Dr. Brian Landrum for reviewing this paper. I would also like to thank Tim Morris for providing the results of the Vicon test. I would also like to thank Dr. Chang-Kwon Kang and Tim Morris for their continued support throughout the research process. Their feedback and wealth of information was invaluable to understanding biological flapping wing dynamics. This study is in part supported by NSF CMMI-1761618.

References

[1] Brower, L. "Monarch Butterfly Orientation: Missing Pieces of a Magnificent Puzzle," *Journal of Experimental Biology*, Vol. 199, pp. 93–103, 1996

[2] Tejaswi, K. C., Madhu Sridhar, Chang-Kwon Kang, and Taeyoung Lee. "Effects of abdomen undulation in energy consumption and stability for monarch butterfly." *Bioinspiration & Biomimetics* (2020)